

## Dimensionality of collective pinning in $2H\text{-NbSe}_2$ single crystals

L. A. Angurel

*Departamento de Ciencia y Tecnología de Materiales y Fluidos, Centro Politécnico Superior, María de Luna, 3,  
E-50015 Zaragoza, Spain*

F. Amin

*Kamerlingh Onnes Laboratory, P.O. Box 9506, 2300 RA Leiden, The Netherlands*

M. Polichetti

*Dipartimento di Fisica, Università di Salerno-INFM, Via S. Allende, Baronissi (SALERNO), I-84081, Italy*

J. Aarts and P. H. Kes

*Kamerlingh Onnes Laboratory, P.O. Box 9506, 2300 RA Leiden, The Netherlands*

(Received 13 February 1997)

ac susceptibility measurements have been used to determine the dimensionality of the collective pinning in  $2H\text{-NbSe}_2$  crystals. We have analyzed the thickness dependence of the critical current versus field [ $J_c(H)$ ] curves for thicknesses between 6 and 166  $\mu\text{m}$ . Down to 15  $\mu\text{m}$   $J_c(H)$  is independent of the thickness showing that the pinning is three dimensional. This is in agreement with estimates from collective pinning theory. Deviations occur for the 6  $\mu\text{m}$  thick sample near the peak-effect regime, possibly indicating a crossover to two-dimensional behavior. In the thicker samples the peak effect clearly cannot be assigned to a dimensional crossover. The frequency dependence reflects a crossover from a Campbell regime to a nonlinear regime related to small flux creep effects. [S0163-1829(97)02830-0]

### I. INTRODUCTION

$$h_0 = 0.971 J_c d \quad (1)$$

ac susceptibility has widely been used for the determination of the critical current density  $J_c$  in superconducting materials. It is complementary to the traditional four-probe transport measurements and is based on the assumption that the flux line arranges itself according to the conditions of the critical state.<sup>1,2</sup> The most common experimental configuration is that of an ac field of amplitude  $h_0$  superimposed to a dc field  $H_{dc}$  which is much larger  $h_0 \ll H_{dc}$ . In this case it is typical to assume that, in the ac loop, the critical current is constant, and only determined by  $H_{dc}$ ,  $J_c = J_c(H_{dc})$ . With this assumption and in absence of demagnetization effects, a maximum in the out-of-phase component of the first harmonic of the ac susceptibility  $\chi''$  is expected when the ac profile reaches the center of the sample. This fact allows us to determine  $J_c(H_{dc})$  from  $h_0$  and the dimensions of the sample perpendicular to the direction of the field.

However, in many cases, the experiments are performed on thin films or single crystals with the field perpendicular to their surface. This arrangement requires an adapted analysis. If the sample is a disk of radius  $r$  and thickness  $d$  ( $d < r$ ), the critical state occurs through the thickness instead of the radius.<sup>3</sup> These demagnetization effects are related with the self-field generated by the induced currents. If the flux has fully penetrated the sample, e.g., after field cooling (FC), these effects are not important in dc magnetization measurements, but they do play a role in ac experiments. The ac susceptibility for a thin circular disk in a perpendicular field has been calculated in recent works.<sup>4-8</sup> Clem and Sánchez<sup>7</sup> showed that the maximum in  $\chi''(h_0)$  for  $H_{dc} = 0$  appears when the relation

is satisfied. It can be easily shown that this relation also applies for  $\chi''(H_{dc})$  at a fixed  $h_0$  ( $h_0 \ll H_{dc}$ ) allowing us to infer  $J_c(H_{dc})$  within a constant of order unity.<sup>4-8</sup> In practice, the critical state model should be corrected in order to include the influence of flux creep.<sup>9</sup> Flux creep phenomena are recognized by the frequency dependence of the ac susceptibility.<sup>10</sup> These effects can be very predominant in high-temperature superconductors.

This thickness dependence of the ac susceptibility can be conveniently used to probe the thickness dependence of  $J_c(H_{dc})$  in layered superconductors in the perpendicular-field geometry, e.g., for the layered compound  $2H\text{-NbSe}_2$ . In this material, the critical current, in the low-field regime, can be described<sup>11,12</sup> by the collective pinning theory of Larkin-Ovchinnikov.<sup>13</sup> In the high-field regime, however, a peak effect (PE) occurs in  $J_c(H_{dc})$  or  $J_c(T)$  close to the critical field line  $H_{c2}(T)$ .<sup>11,14,15</sup> Different scenarios have been suggested for the PE: (i) a sudden softening of the elastic moduli on going from local to nonlocal elasticity,<sup>13</sup> (ii) a dimensional crossover from two-dimensional (2D) to 3D collective pinning,<sup>11</sup> (iii) a melting transition of the vortex lattice at the onset of the peak,<sup>16</sup> or (iv) at the maximum of the PE.<sup>17,18</sup> In this paper we are not considering the origin of the PE, but we concentrate on the dimensionality of the collective pinning in the field regime below the PE, which is nonetheless relevant for (i) and (ii). The thickness dependence of  $J_c(H_{dc})$  determines the dimensionality; for 3D collective pinning,  $J_c$  should be thickness independent, while for 2D collective pinning a  $d^{-1}$  dependence is expected.

In this work, we have measured  $\chi_{ac}(H_{dc}, h_0)$  on a

$2H\text{-NbSe}_2$  single crystal with  $d=166\ \mu\text{m}$ , which is expected to be in the 3D regime. These measurements were repeated after cleaving the same crystal several times to explore the influence of the thickness without modifying the transverse dimensions. An additional advantage of inductive methods over transport techniques is that the problems related with contacts and self-heating are avoided.<sup>19</sup> On the other hand, the analysis of  $\chi_{ac}(H_{dc}, h_0)$  is complicated by the frequency dependence, which is equivalent to the choice of the voltage criterion for  $J_c$  in transport experiments. To analyze the effects related to flux creep, the frequency dependence was studied on two other crystals with different thicknesses, but with approximately the same transverse dimensions.

## II. EXPERIMENTAL

All measurements have been performed on disk-shaped samples. The thickness of the samples was determined by measuring their surface area and weighing the samples in a microbalance. The higher errors arise from the surface area and have been estimated to introduce uncertainty in the thickness of  $2\ \mu\text{m}$ . To determine the density, the lattice parameters and the crystal structure presented in Ref. 20 have been used, giving a value of  $6.44 \times 10^3\ \text{kg/m}^3$ .

Three different samples have been used to perform this study. The influence of the thickness has been analyzed on a sample with a diameter of 1.68 mm (sample A). Its initial thickness was  $d=166\ \mu\text{m}$  and it was repeatedly cleaved sandwiching it between tape strips.<sup>11</sup>  $\chi_{ac}$  measurements, at a frequency of 1300 Hz, with different  $h_0$  and fixed temperatures (4.24 and 5.73 K), were performed for six different thicknesses ranging between 166 and  $15\ \mu\text{m}$ : 166, 122, 83, 66, 32, and  $15\ \mu\text{m}$ . The samples were cooled down in zero field and both the dc field and ac field were applied perpendicular to the sample surface. In some cases,  $\chi_{ac}(T)$  measurements have been done cooling down in field or  $\chi(H_{dc})$  has been recorded from high field to low field. The results were the same, showing that these experiments do not show any history dependence. The sample of  $15\ \mu\text{m}$  was cleaved again obtaining a sample with a thickness of around  $6\ \mu\text{m}$ , as determined by scanning electron microscopy.

The frequency dependence has been studied in two different crystals with similar dimensions. Sample B had a thickness of  $110\ \mu\text{m}$ . It was measured in a superconducting quantum interference device system (Quantum Desing) at 4.45 K and at frequencies of 1, 119, and 987 Hz. The last one (sample C) had a thickness of  $26\ \mu\text{m}$  and the measurements were performed at 4.24 K in an ac susceptometer using the frequencies of 130 Hz, 1.3 kHz, and 13 kHz. Sample A after each cleavage and samples B and C were initially characterized measuring  $\chi(T, H_{dc}=0)$  in order to determine their critical temperature. In all cases, a  $T_c \approx 7.1\ \text{K}$  is obtained without showing any thickness dependence, as was expected.

## III. RESULTS AND DISCUSSION

### A. Determination of $J_c(H_{dc})$ from ac susceptibility

The typical  $\chi(H_{dc})$  curves for different ac fields at  $\nu=1\ \text{Hz}$  and  $T=4.45\ \text{K}$  for sample B are presented in Figs. 1 and 2. The data have been scaled in order to yield an in-phase

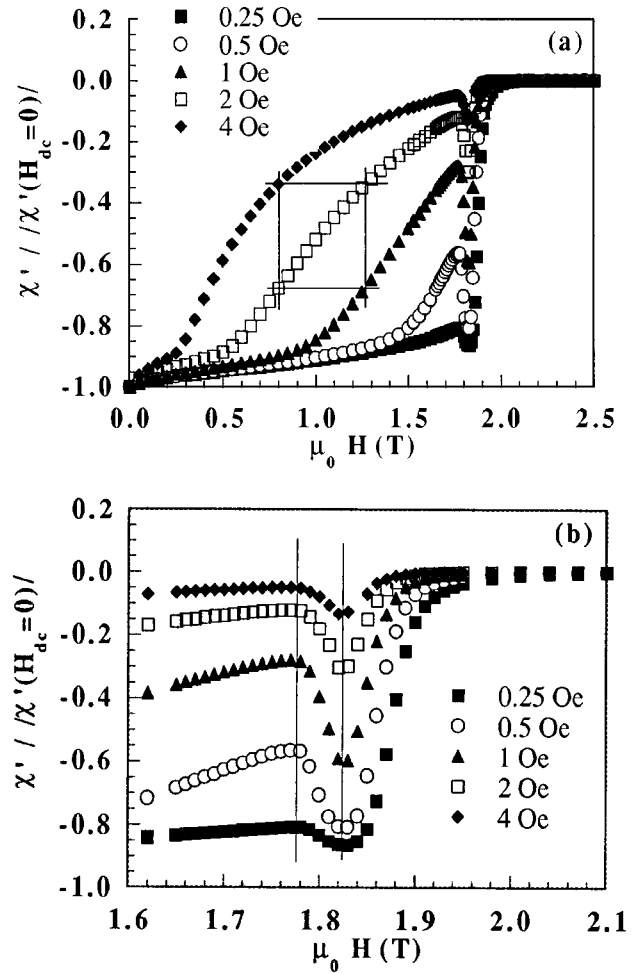


FIG. 1. (a) Isothermal in-phase ac susceptibility component  $\chi'(H_{dc})$  for sample B using different ac fields ( $T=4.45\ \text{K}$ ,  $\nu=1\ \text{Hz}$ ). The meaning of the rectangle depicted in the figure is presented in the text. (b) Detail of the region close to the peak effect. The two lines indicate the position of  $H_{\text{onset}}$  and  $H_{\text{peak}}$ .

component  $\chi' = -1$  at zero dc field. The following features can be observed in the behavior of  $\chi'$ .

(i) After a kink in  $\chi' = -(0.85-0.9)$  the behavior follows the predictions of the critical state models. The curves are strongly  $h_0$  dependent, which suggests that the most important contribution to losses is hysteretic. As proposed by Civale *et al.*,<sup>21</sup> this assumption can be confirmed performing measurements for several ac field amplitudes varying in the ratio 1:2:4:8:⋯ and inscribing rectangles as shown in Fig. 1(a). This interpretation is based on the idea that the value of  $\chi'$  (horizontal lines in the rectangle) is a measure of how far the ac profile has penetrated inside the sample. This is not the only contribution because as we are going to show later, there is also a small frequency dependence.

(ii) There is a field  $H_{\text{onset}}$  at which  $|\chi'|$  shows a minimum. In Fig. 1(b), a blow-up of the region near this field is presented. From these curves we observe that, at least within the range of  $h_0$  we have used,  $H_{\text{onset}}$  is independent of  $h_0$ , while the corresponding value of  $\chi'$ ,  $\chi'_{\text{onset}}$ , does depend on it.

(iii) Before reaching  $H_{c2}$ , defined as the field at which  $\chi'$  starts to deviate from zero with the lowest ac field, a minimum in  $\chi'$  occurs at a field  $H_{\text{peak}}$ . In a similar way to the previous point, the value of  $h_0$  modifies the value of  $\chi'$  at the

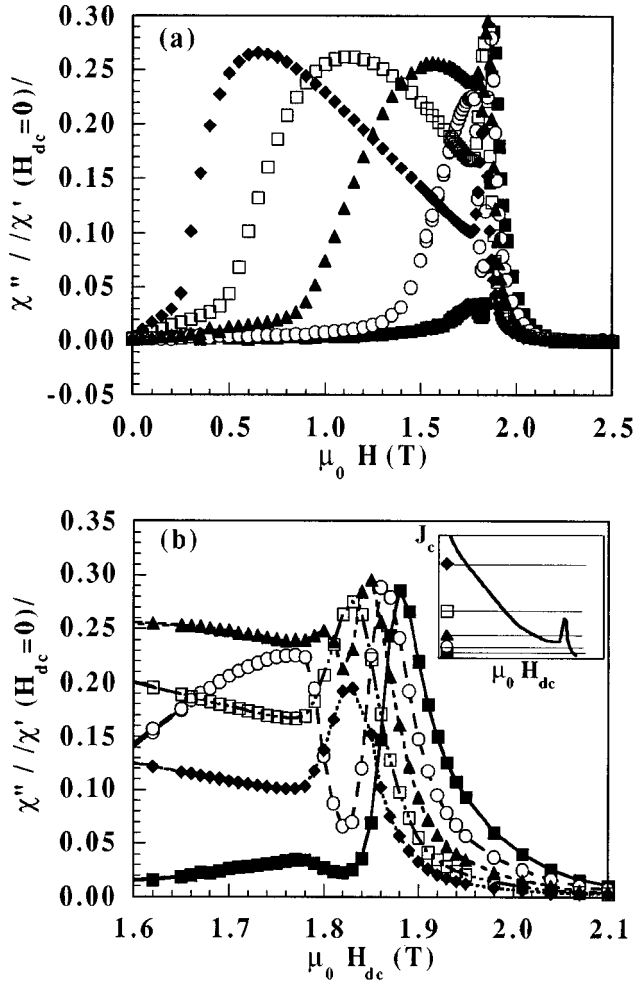


FIG. 2. (a) Isothermal out-of-phase ac susceptibility component  $\chi''(H_{dc})$  for sample B using different ac fields ( $T=4.45$  K,  $\nu=1$  Hz). (b) Detail of the region close to the peak effect. The lines are guides to the eye. The inset shows the level of the currents that are induced in each of the five previous curves when the maxima are reached (same symbols as in Fig. 1).

minimum  $\chi'_{\text{peak}}$  but not  $H_{\text{peak}}$ . For all our measurements, we find that  $H_{\text{peak}}$  is related to  $H_{c2}$ , i.e.,  $h_{\text{peak}}=H_{\text{peak}}/H_{c2}=0.86$ .

If the measurements are performed at different temperatures, this relation also holds. For the temperature range of our experiments, the  $H_{\text{peak}}(T)$  dependence is linear and can be fitted with the expression (SI units)

$$\mu_0 H_{\text{peak}} = 4.81 - 0.676 T. \quad (2)$$

This linear dependence has been previously reported by D'Anna *et al.*<sup>14</sup> If we combine this behavior with the fact that  $h_{\text{peak}}(T)$  is constant, a linear relation between  $H_{c2}$  and the temperature should be expected and the slope of this line should be  $-\mu_0(dH_{c2}/dT)=0.786$  T/K. This value is very close to the values reported from magnetization measurements in the initial studies performed on 2H-NbSe<sub>2</sub> using a similar geometry.<sup>22</sup>

Looking at the  $\chi''(H_{dc})$  curves displayed in Fig. 2, we discriminate, depending on  $h_0$ , between different multippeak structures.<sup>23,24</sup> It is necessary to determine if these peaks represent the fact that the condition associated with Eq. (1) is

fulfilled, as it is the case of the broad maximum below  $H_{\text{onset}}$  or if the peak is only an evidence of the fact that the  $J_c(H_{dc})$  dependence shows a maximum. In this second case, Eq. (1) cannot be applied and, consequently, these peaks cannot be used to determine  $J_c$ . The different cases that are reported in this kind of experiment can be explained by considering a monotonously decreasing  $J_c(H_{dc})$  dependence followed by a peak effect at  $H_{\text{onset}}$ , see inset Fig. 2(b).

(i) With very low ac fields (curves of 0.25 and 0.5 Oe in Fig. 2), the current we are inducing with the ac field is lower than the minimum in  $J_c(H_{\text{onset}})$ . Therefore, the peak effect region is reached before the relation  $h_0=0.971J_c d$  is fulfilled. In this case,  $\chi''(H_{dc})$  increases until the onset of the peak effect, then decreases and shows a minimum very close to  $H_{\text{peak}}$ . Above this field, it shows a large maximum at the field where the steeply descending  $J_c(H_{dc})$  curve is crossed [see inset Fig. 2(b)].

(ii) With high ac fields the critical current is higher than the maximum of the peak effect. It is seen that  $\chi''(H_{dc})$  shows two maxima (curves of 2 and 4 Oe). The broad peak at low dc fields corresponds to the peak which is expected in critical state models and allows to determine  $J_c$ . At high dc fields there is an additional peak which is not a peak in the sense of the critical state, i.e., at which Eq. (1) is fulfilled, it merely reflects the PE observed in the  $J_c(H_{dc})$  dependence. The position of this second peak is closely related with the position of the minimum in  $\chi'(H_{dc})$  and hence it is independent of  $h_0$ .

(iii) There is an intermediate range of fields in which  $\chi''(H_{dc})$  shows three peaks, and for all of them Eq. (1) holds (curve of 1 Oe in Fig. 2).

When the thickness of the sample is reduced the important trends previously mentioned appear at very low  $h_0$  values. In these situations, the noise in the  $\chi''$  curves at high fields becomes predominant and it is difficult to classify a given curve. For this reason, it is important to obtain additional information from the values of  $\chi'$  at the fields where characteristic features occur. They allow us to more precisely define the values of  $J_c$  at  $H_{\text{onset}}$  and  $H_{\text{peak}}$  and to classify a given curve. We have previously mentioned that  $\chi'_{\text{onset}}$  and  $\chi'_{\text{peak}}$  are functions of  $h_0$ . In addition, the critical state model predicts a specific combination (depending on the actual geometry of the sample) of  $\chi'$  and  $\chi''$  for the field  $H_{dc}(h_0)$  at which Eq. (1) is fulfilled. In our geometry the value for  $\chi'$  is  $\approx -0.46$  at the broad, low-field peak in  $\chi''$ , with a small correction associated with  $h_0$  and the frequency of the ac field. Therefore,  $J_c(H_{\text{onset}})$  can be deduced from the ac field at which  $\chi'_{\text{onset}}=-0.46$ . With lower  $h_0$  values the broad, low-field peak in  $\chi''$  does not appear and the curves correspond to case (i). On the contrary, the high-field peak in  $\chi''$  appears at  $\chi' \approx -0.40$ , thus  $J_c(H_{\text{peak}})$  can be obtained from the ac field at which  $\chi'_{\text{peak}}=-0.40$ . At this  $h_0$  value the boundary between cases (ii) and (iii) is reached.

## B. Thickness dependence

Once we learned how to extract information from these measurements, we studied the influence of the sample thickness. Figure 3 shows the thickness dependence of  $\chi'$  for a given  $h_0$ , in this case 2.08 Oe ( $T=4.2$  K). Only sample A was used and only the thickness was modified while the

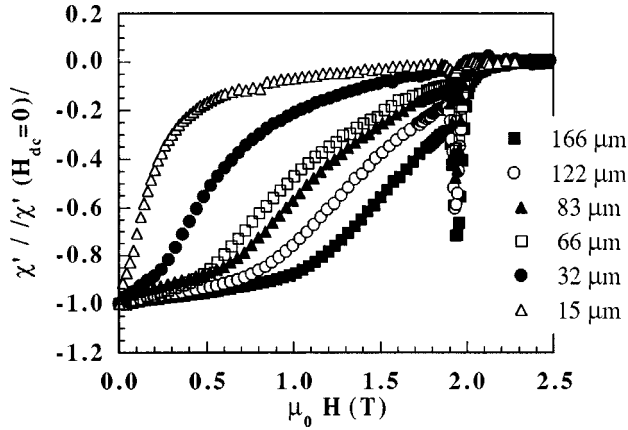


FIG. 3. Thickness dependence of  $\chi'(H_{dc})$  ( $h_0=2.08$  Oe,  $T=4.24$  K,  $\nu=1300$  Hz) in sample A.

transverse dimensions were not altered. The thinner the sample, the faster the field penetrates and the lower the values of  $|\chi'_{onset}|$  and  $|\chi'_{peak}|$ . The effect of reducing the thickness is equivalent to increasing  $h_0$ . In fact, the parameter that controls the shape of the curves is the ratio between  $h_0$  and the thickness. For instance, if the curve of 2.08 Oe for the sample which is 166  $\mu\text{m}$  thick and the curve of 1.04 Oe for the sample of 83  $\mu\text{m}$  are compared, they coincide because the ratio  $h_0/d$  is the same.

Using Eq. (1),  $J_c(H_{dc})$  has been determined and the data are presented in Fig. 4. In the inset, the region near the peak is presented in more detail. The results resemble those obtained in transport measurements on thick samples.<sup>25</sup> In both cases the ascending branch of the peak is very sharp and the value at the peak is almost 3.5 times the value at the onset. The values  $J_c(H_{onset})$  and  $J_c(H_{peak})$  coincide with those obtained from the analysis of  $\chi'_{onset}(h_0)$  and  $\chi'_{peak}(h_0)$ , in this case  $J_c(H_{onset}) \approx 0.68 \times 10^6$  A/m<sup>2</sup> and  $J_c(H_{peak}) \approx 2.34 \times 10^6$  A/m<sup>2</sup>. The results of the samples with thicknesses of 15 and 6  $\mu\text{m}$  are not shown in the PE region because the noise in this region of the  $\chi''$  curves is too large. Instead, some information will be extracted from the  $\chi'$  data.

The most important result of our experiments is that the critical current turns out to be thickness independent show-

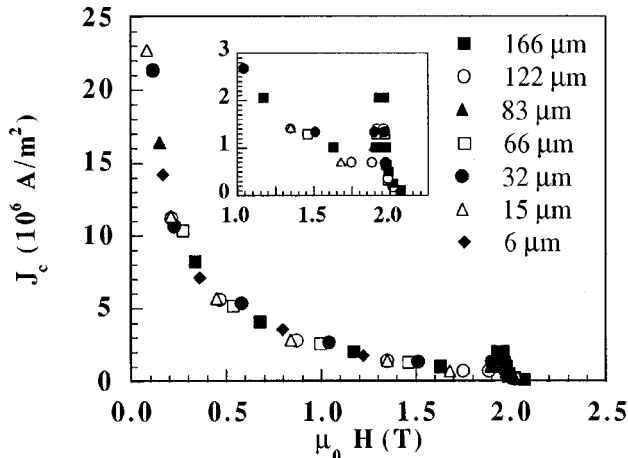


FIG. 4. Field dependence of the critical current obtained from the position of the peaks in  $\chi''(H_{dc})$ . In the inset, the region close to the PE is presented.

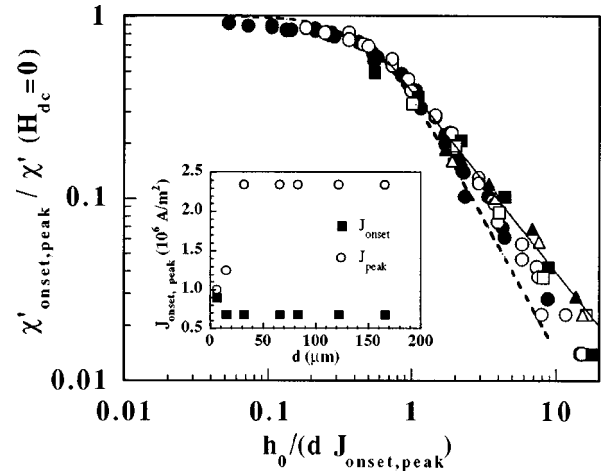


FIG. 5. Scaling of  $\chi'_{peak}$  (open symbols) and  $\chi'_{onset}$  (solid symbols) for the samples with thicknesses between 166 and 32  $\mu\text{m}$  (circles), 15  $\mu\text{m}$  (squares), and 6  $\mu\text{m}$  (triangles). The values used for  $J_{onset}$  and  $J_{peak}$  to get the scaling behavior, are presented in the inset. The meaning of the lines has been explained in the text.

ing that in our NbSe<sub>2</sub> samples the pinning has a 3D character, down to a thickness of 6  $\mu\text{m}$ . The  $J_c$  values we obtained are five times higher than the typical values given in Ref. 15, but similar to results of transport measurements on samples of the same batch.<sup>26</sup> These high values of  $J_c$ , and therefore of the pinning force, have reduced the thickness at which the transition between 3D and 2D collective pinning is expected to occur.

The data presented above demonstrate that in the geometry of our experiment the behavior of the ac susceptibility is determined by the thickness instead of by the radius. In a similar way, the value of  $\chi'$ , which is related with the penetration of the ac profile, in this geometry should depend on the product  $Jd$ . This expectation can be checked by studying the scaling of  $\chi'$  as a function of  $h_0/(dJ)$  for some typical situations. This is done for  $\chi'_{peak}$  and  $\chi'_{onset}$  in Fig. 5. Circles have been used for the measurements performed on the samples with thicknesses between 166 and 32  $\mu\text{m}$ , whereas squares denote the results for 15  $\mu\text{m}$  and triangles for 6  $\mu\text{m}$ . The uniform behavior is nicely seen and displays a change from almost perfect screening [ $\chi'/\chi'(0)=1$ ] to almost total penetration. Such scaling behavior has been predicted in Refs. 7 and 5. The dashed line represents the formulas [Eqs. (31) and (32)] given by Clem and Sánchez.<sup>7</sup> The limiting behavior for large  $h_0$  is  $\chi' \propto h_0^{-3/2}$ . It seems that the dependence  $\chi' \propto h_0$ , as suggested by Zhu *et al.*<sup>6</sup> and given by the drawn line, fits the data better. However, one should keep in mind that the effect of flux creep (see below) will always give rise to larger  $\chi'$  values than those predicted for the critical state model. Therefore, we conclude that our data support Clem's analysis and is at variance with the claim of Ref. 6.

In the inset of Fig. 5 the experimental values of  $J_{onset}$  and  $J_{peak}$  that were used in the scaling plot, are shown as a function of thickness. Down to 32  $\mu\text{m}$  they do not depend on  $d$ , but at 15  $\mu\text{m}$  deviations start to appear.  $J_{onset}$  still has the same value, but a lower  $J_{peak}$  is needed showing that the PE is reduced in this sample. This is even more evident in the 6  $\mu\text{m}$  sample. In this case the deviation appears both at the

onset and at the peak as a signal that the peak in  $J_c(H)$  starts to reduce. Similar behavior is observed in transport measurements.<sup>25</sup> We think it indicates the transition to the 2D regime. In 2D  $J_c$  increases if the thickness is reduced and that is just what is seen for  $J_{\text{onset}}$  which for the 6  $\mu\text{m}$  sample is larger than for the thicker samples. Also the peak effect is less pronounced in 2D. Combining these observations with those of Fig. 4, we conclude that at low fields the sample of 6  $\mu\text{m}$  is in a 3D pinning regime, while it changes to 2D behavior at high fields, especially near the PE where a thickness dependence starts to be observed.

The same studies have been performed at 5.73 K. The curves of  $J_c/(1-T/T_c)$  vs  $H/H_{c2}$  obtained at these two temperatures coincide showing that in this range of temperatures the temperature and field dependence of  $J_c$  can be expressed as  $J_c(T,H)=f(h)(1-t)$  where  $h=H/H_{c2}(T)$  and  $t=T/T_c$ .

### C. Collective pinning analysis

Having established that the pinning in our crystals is of a 3D nature, it is interesting to make some estimates of the transverse and longitudinal pinning correlation lengths (Larkin lengths)  $R_c$  and  $L_c$ .<sup>13</sup> We carry out this analysis for the results at  $T=4.24$  K only and start by first determining the pinning strength  $W$  from the low-field limit of the critical current,  $J_c(0)$ . From separate transport measurements<sup>26</sup> it was found that  $J_c(0)\approx 5\times 10^7$  A/m<sup>2</sup> at 5 mT which compares very well with the value reported by Duarte *et al.*<sup>12</sup> At low fields the vortices are assumed to be independently pinned by the collective interaction with the pinning centers, i.e.,  $R_c(0)\approx a_0$  and  $L_c(0)\approx \xi[J_0(T)/J_0(0)]^{1/2}/\gamma$ .<sup>27</sup> Here  $J_0(T)$  is the depairing current density and  $\gamma$  the anisotropy parameter. In the following, numerical estimates are made by taking  $\xi(0)=7.8$  nm,  $\lambda_L(0)=205$  nm (determined from the reversible magnetization of NbSe<sub>2</sub> crystals of the same batch<sup>25</sup>),  $\mu_0 H_c=92$  mT,  $J_0=2.1\times 10^{11}$  A/m<sup>2</sup>, and  $\gamma=3.0$  [determined from the angular dependence of the torque near  $T_c$  (Ref. 28)]. To obtain the values of these parameters at  $T=4.24$  K we used the Ginzburg-Landau temperature dependences  $\xi(T)=\xi(0)/(1-t)^{1/2}$ ,  $\lambda(T)=\lambda_L(0)/[2(1-t)]^{1/2}$  and  $J_0(T)=J_0(1-t)^{3/2}$ . After substitution we find  $L_c(0)\approx 0.14$   $\mu\text{m}$ . Assuming that the field dependence of  $W$  is given by  $W=W_0 b(1-b)^2$  with  $b=B/\mu_0 H_{c2}$ , we can determine the parameter  $W_0$  from the expression for single vortex pinning, namely,

$$W_0\approx L_c(0)J_c^2(0)\phi_0\mu_0 H_{c2}, \quad (3)$$

and obtain  $W_0\approx 1.3\times 10^{-6}$  N<sup>2</sup>/m<sup>3</sup>.

Next we assume that  $R_c>\lambda_h$  [ $=\lambda/(1-b)^{1/2}$ ] so that the dispersion of the tilt modulus  $c_{44}(=B^2/\mu_0)$  can be ignored and  $R_c$  is given by<sup>13</sup>

$$R_c\approx \left[ \frac{W}{8\pi c_{66}^{3/2} c_{44}^{1/2}} \right]^{-1} \frac{a_0^2}{4}. \quad (4)$$

Here  $c_{66}$  is the shear modulus given by  $c_{66}\approx (\phi_0 B/16\pi\mu_0\lambda^2)(1-b)^2$  and  $a_0$  is the vortex lattice parameter. After substitution we obtain

$$R_c\approx \frac{(\phi_0^4 b^{1/2}(1-b))}{(64\pi^2\sqrt{2}\mu_0^2\lambda^3\xi^3W_0)} = \frac{\pi^2(\mu_0 H_c^2)^2\lambda\xi}{\sqrt{2}W_0} b^{1/2}(1-b), \quad (5)$$

which yields  $R_c\approx 0.45b^{1/2}(1-b)$  m.  $L_c$  in the nondispersive regime follows from

$$L_c\approx \left( \frac{c_{44}}{c_{66}} \right)^{1/2} R_c = 2\sqrt{2} \frac{\lambda R_c b^{1/2}}{\xi(1-b)}, \quad (6)$$

which gives  $L_c\approx 24b$  m. For relevant values of  $b$  the above results imply that the vortex lattice would be perfect throughout the entire sample if the dispersion of  $c_{44}$  is neglected, and  $J_c$  would be many orders of magnitude smaller than our experimental values, namely,  $J_c\approx (2.4\times 10^{-4}/b^{3/2})$  A/m<sup>2</sup>.

*This example clearly shows that the Larkin lengths should be determined by taking into account the dispersion of  $c_{44}$ .* For anisotropic superconductors  $c_{44}(k_\perp, k_z)=c_{44}/(1+\lambda_h^2 k_z^2 + \gamma^2 \lambda_h^2 k_\perp^2)$ , where  $k_\perp$  and  $k_z$  are wave vectors describing the deformation fields normal and parallel to the field direction, respectively.<sup>27</sup> The most relevant wave vectors<sup>29</sup> take on the values  $k_\perp\approx \pi/R_c$  and  $k_z\approx \pi/L_c$ . As we will see below,  $L_c\gg R_c$ , and therefore  $c_{44}(k_\perp)=c_{44}R_c^2/(\pi\gamma\lambda_h)^2$ . We thus obtain

$$L_c\approx \left( \frac{c_{44}(k_\perp)}{c_{66}} \right)^{1/2} R_c = \left( \frac{2\sqrt{2}\kappa}{\pi\gamma} \right) \left( \frac{b}{(1-b)} \right)^{1/2} \frac{R_c^2}{\lambda}, \quad (7)$$

where  $\kappa(=\lambda/\xi)$  is the Ginzburg-Landau parameter. The Larkin lengths are now easily determined from the Larkin-Ovchinnikov expression  $J_c B=(W/R_c^2 L_c)^{1/2}$ . The results obtained by using the  $J_c$  values of Fig. 4 are shown in Fig. 6 for fields up to  $H_{\text{peak}}$ .

It follows from these estimates that the vortex lattice is highly disordered. The sharp decrease of  $L_c$  and  $R_c$  between  $H_{\text{onset}}$  and  $H_{\text{peak}}$  indicates that the correlated volume collapses very fast, much faster than  $W_0$ , which causes the increase of  $F_p$  and  $J_c$ . Both at low fields and at  $H_{\text{peak}}$ ,  $R_c$  approaches its lowest limit  $R_c\approx a_0$ . The value of  $L_c$  is seen to be much smaller than the sample thickness, even for  $d=6$   $\mu\text{m}$ , see Fig. 6(b). A transition to 2D behavior is predicted when  $L_c=d/2$ .<sup>30</sup> Since the maximum value of  $L_c$  is of the order of 1  $\mu\text{m}$ , a dimensional crossover is not to be expected for our samples. However, it should be noted that numerical factors of order unity have been omitted from the expressions in the review of Blatter *et al.*<sup>27</sup> Keeping these factors would increase the estimate for  $L_c$  by about a factor of 2. It may therefore be that the deviating behavior of our 6  $\mu\text{m}$  thick sample at high fields is an indication for 2D collective pinning. In addition, the field dependence of  $L_c$  could explain why this sample seems to be in 3D at low fields and in 2D near the PE. Another interesting point to note is that the critical current in the NbSe<sub>2</sub> crystals used in the work of Battacharya and Higgings<sup>18</sup> is two to three orders of magnitude smaller than the  $J_c$ 's in our crystals. It is therefore quite likely that the pinning for the perpendicular field configuration in Ref. 18 is of 2D nature, in which case  $R_c$  follows from

$$R_c = \frac{(W/d)^{1/2}}{J_c B}. \quad (8)$$

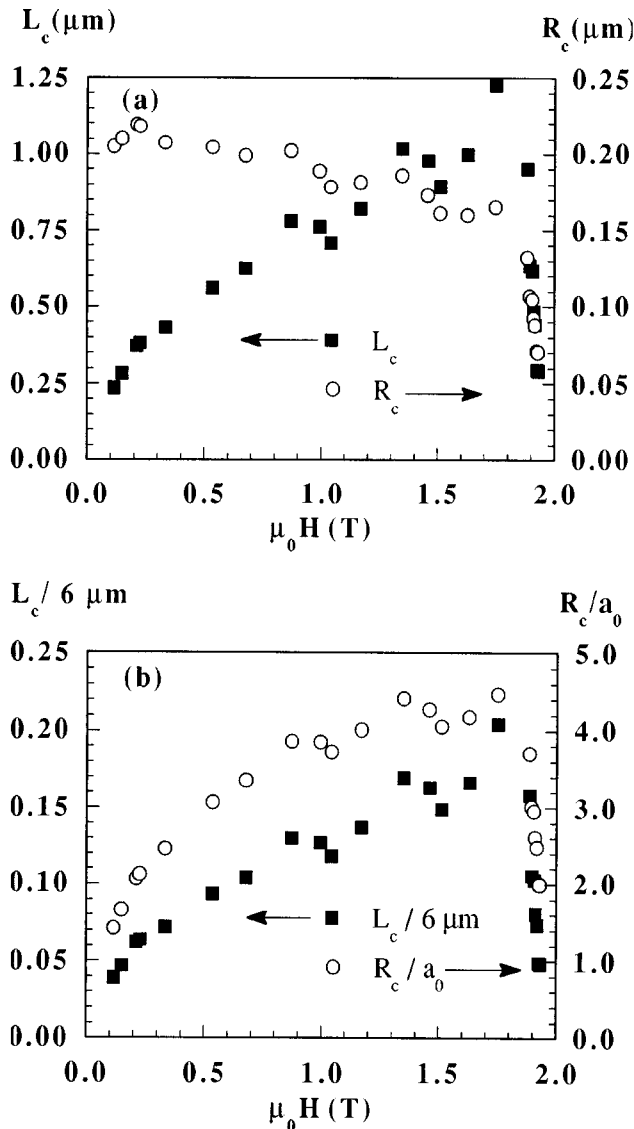


FIG. 6. (a) Computed values of the characteristic lengths  $L_c$  and  $R_c$  obtained using Eq. (7) and the data of Fig. 4. (b) Ratios  $L_c/d$ , with  $d=6 \mu\text{m}$ , and  $R_c/a_0$ .

The pinning strength should again be determined from the low-field value of  $J_c$ . Finally, it is clear that the peak effect in our samples thicker than  $6 \mu\text{m}$  is not related to a dimensional crossover of the pinning. It is more likely to be related to the transition from a vortex glass to a vortex liquid. In view of the relatively large disorder this transition is not expected to be a real phase transition (melting). It rather is a crossover which is characterized by a steep decay of the shear modulus starting at  $H_{\text{onset}}$ . It causes the sudden increase of  $J_c$  related to the lattice softening. At  $H_{\text{peak}}$   $R_c \approx a_0$  which supports the view that at  $H_{\text{peak}}$  the shear modulus has gone to zero and the transition to the liquid has been completed.<sup>31,17</sup>

#### D. Frequency dependence

The influence in the above conclusions of the choice of a particular frequency has been analyzed in samples B and C. Both samples exhibit similar characteristics. In Fig. 7 the behavior of  $\chi_{\text{ac}}(H_{\text{dc}})$  for sample B, at  $T=4.45 \text{ K}$  and with

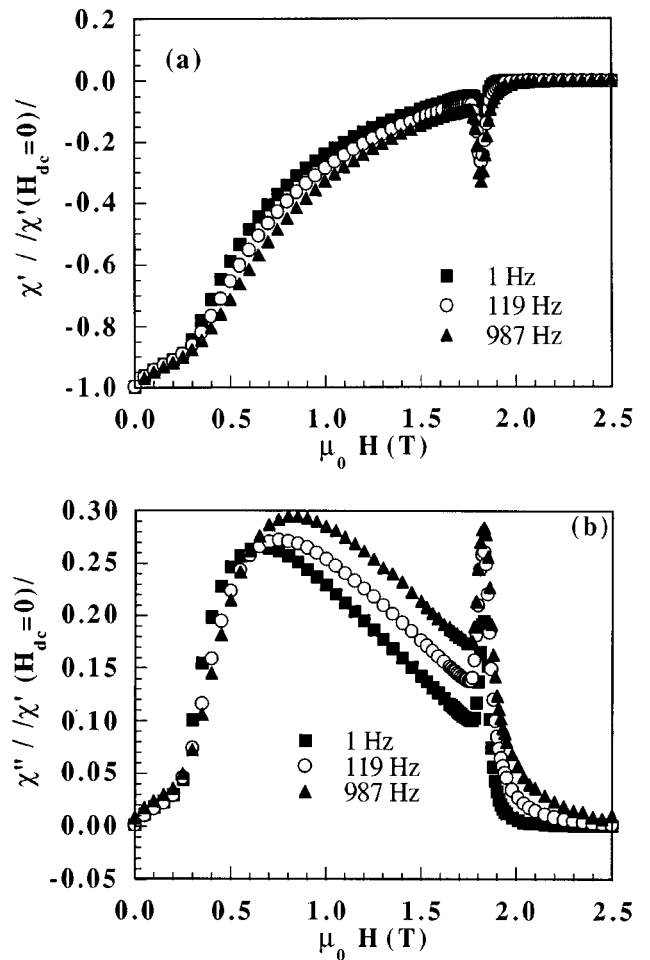


FIG. 7. Frequency dependence of (a)  $\chi'(H_{\text{dc}})$  and (b)  $\chi''(H_{\text{dc}})$  for sample B at  $T=4.45 \text{ K}$  and  $h_0=4 \text{ Oe}$ .

$h_0=4 \text{ Oe}$ , is depicted for different frequencies (1, 119, and 987 Hz). It is possible to distinguish between two regions: one at low dc fields where the curves are frequency independent and a second region, after a change in the slope of the curves, in which this frequency dependence is evident.

#### 1. Nonlinear regime

Although the results presented in Fig. 1 pointed out that most of the losses are hysteretic, small corrections due to the frequency dependence, associated with flux creep, should be included. These corrections have been evaluated for sample C in the range of frequencies between 130 Hz and 13 kHz. From the analysis of the curves of  $\chi''(H_{\text{dc}})$  the dependence of  $J_c$  on the reduced dc field  $h$  has been extracted and is shown in Fig. 8. From this figure we can see that the critical currents have the same kind of dependence on  $H_{\text{dc}}$  for all the frequencies analyzed, and that the particular values do not differ too much from one frequency to the other. The biggest differences, around a 20%, appear in the region of intermediate fields; after the PE these differences are negligible. From these results we conclude that the choice of a particular frequency does not essentially influence the results of our analysis at different thicknesses. The order of magnitude of  $J_c$  is correct and the above conclusions for the 3D behavior of the samples still remains valid.

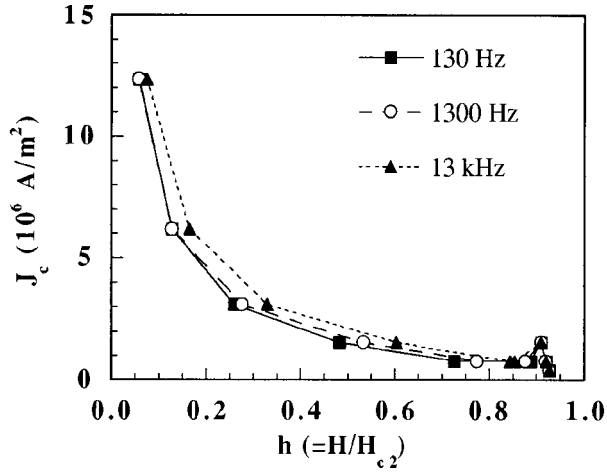


FIG. 8. Influence of the frequency on the  $J_c(H_{dc})$  curves measured for sample C at  $T=4.24$  K.

### 2. Linear behavior: Campbell regime

The initial frequency independent region has been associated with the Campbell regime. The ac response of the system at low ac amplitudes is determined by vortex oscillations near equilibrium. The vortices make small excursions from their local potential minima, which allows us to assume that the potential is harmonic and the restoring force elastic. A small uniform displacement  $\mathbf{u}$  causes a restoring force  $F(\mathbf{u}, \mathbf{r}) = -\alpha_L \mathbf{u}(\mathbf{r})$ , where  $\alpha_L$  is the Labusch constant.<sup>32</sup> In this situation, the penetration depth of the ac field is real and frequency independent and it is given by<sup>33</sup>

$$\lambda_C = \left( \frac{B^2}{\mu_0 \alpha_L} \right)^{1/2}. \quad (9)$$

The behavior is similar to a Meissner state but with a larger penetration depth. The crossover from the Campbell regime to nonlinearity takes place when  $h_0$  takes the value

$$h_C = J_c \lambda_C = \left( \frac{B J_c r_f}{\mu_0} \right)^{1/2}, \quad (10)$$

where we used that  $\alpha_L = F_p / r_f = J_c B / r_f$ ,  $r_f$  being the range of the pinning potential.

A detailed study of the Campbell regime has been performed for sample B by carrying out  $\chi_{ac}(h_0)$  measurements at fixed dc fields, see Fig. 9. The Campbell regime is observed at low amplitudes where  $\chi'$  is independent of  $h_0$  and  $\chi''$  is nearly zero. The Campbell penetration depth can be obtained from the value of  $\chi'$  in this region. Considering the geometry of a disk of radius  $R$  and thickness  $d$  in a transverse field,  $\lambda_C$  follows from<sup>34</sup>

$$\mu' = 1 + \chi' \approx \frac{6\lambda_C^2}{\pi R d} \ln \left( 11.3 \frac{R d}{2\pi\lambda_C^2} \right). \quad (11)$$

Figure 10(a) shows the dependence  $\lambda_C^2(H_{dc})$  obtained from the constant values of  $\chi'$  and using Eq. (11). In addition, the values of  $\alpha_L$ , obtained using Eq. (9) and assuming that  $B = \mu_0 H$ , are depicted. It can be observed that these values are of the right order of magnitude. In Fig. 10(b) we compare the values of  $h_C$  (obtained from the measurements

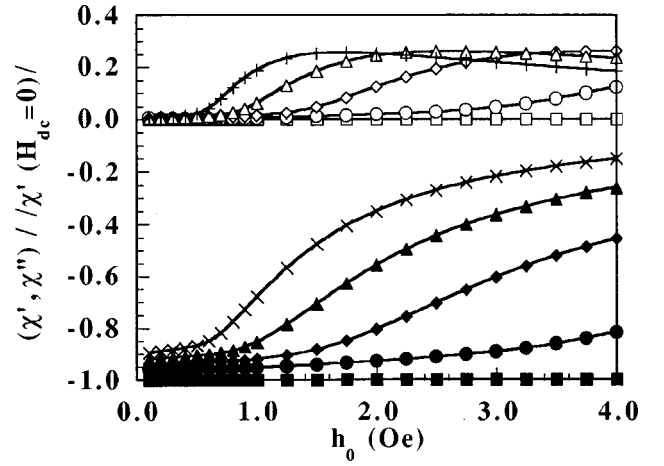


FIG. 9. Isothermal behavior of  $\chi'(h_0)$  and  $\chi''(h_0)$  for sample B at  $T=4.45$  K,  $\nu=1$  Hz and different  $\mu_0 H_{dc}$ ; 0 T (squares), 0.3 T (circles), 0.6 T (rhombus), 0.9 T (triangles), and 1.2 T (crosses). The lines are guides to the eye.

by taking the  $h_0$  value where  $\chi''$  starts to deviate from zero) and the values of  $J_c \lambda_C$ , where  $J_c$  is the critical current density at this temperature determined at the same frequency. It can be observed that the agreement between both values is reasonable.

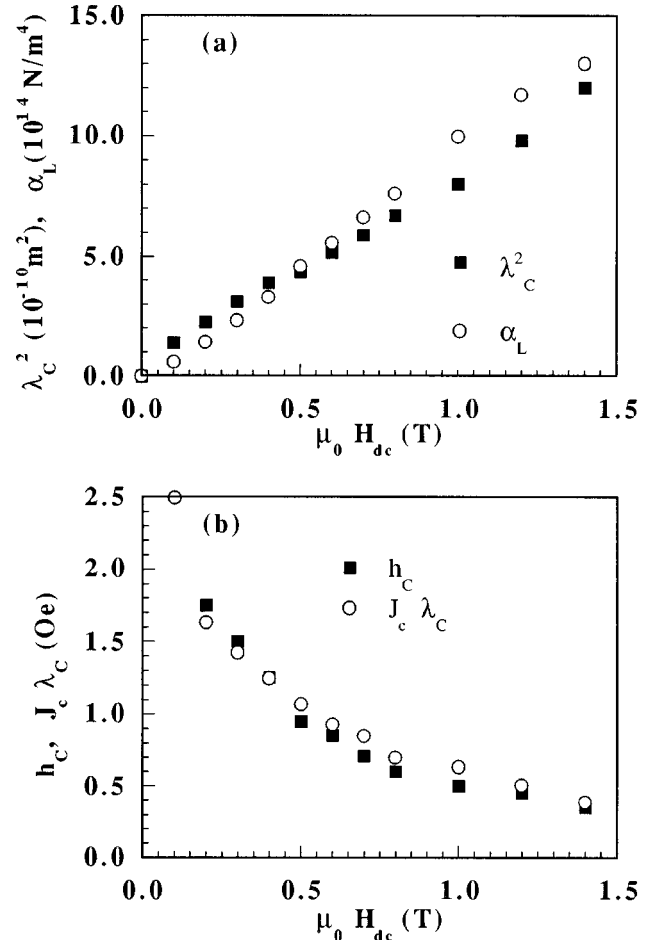


FIG. 10. (a)  $H_{dc}$  dependence of  $\lambda_C^2$  and  $\alpha_L$ . (b) Comparison of the  $H_{dc}$  dependence of  $h_C$  determined from  $\chi_{ac}(h_0)$  measurements and the product  $J_c \lambda_C$ .

With these results, an estimation of  $r_f$  can be made as well. We find that  $r_f$  changes from 29 nm at  $\mu_0 H_{dc}=0.2$  T ( $b \approx 0.1$ ) to 2 nm at  $\mu_0 H_{dc}=1$  T ( $b \approx 0.5$ ).  $r_f$  is of the right order of magnitude, namely about  $\xi$  at low fields (in  $2H$ -NbSe<sub>2</sub>,  $\xi=12.1$  nm at 4.45 K), but the field dependence of  $r_f$  is not yet understood. It may indicate that  $r_f$  is determined by the transition from elastic to plastic behavior at higher fields.

#### IV. CONCLUSIONS

This work provides experimental evidence that in transverse geometry the important sample dimension for the penetration of the field is the thickness of the sample, in agreement with recent works in which critical state models have been developed for this geometry. Applying these ideas, it has been demonstrated that ac susceptibility is a useful technique to determine the dimensionality of the collective pinning in  $2H$ -NbSe<sub>2</sub> crystals. It has been shown that in the range of thicknesses studied, the  $J_c(H)$  curve does not depend on the thickness which allows us to affirm that the collective pinning in these samples is 3D. Only the sample with a thickness of 6  $\mu\text{m}$  shows a deviation from this behav-

ior at high fields, near the peak effect. The Larkin lengths have been estimated by assuming an aspect ratio of the Larkin domain which explicitly takes into account the dispersion of the tilt modulus. It follows that the vortex lattice is highly disordered and that a crossover from a vortex glass to a vortex liquid takes place between  $H_{\text{onset}}$  and  $H_{\text{peak}}$ .

It has been shown that the previous conclusions do not depend significantly on the frequency, because changing the frequency from 130 Hz to 13 kHz leads to an up-shift of  $J_c$  over at most 20%. In the study of the frequency dependence a regime has been identified in which the susceptibility is frequency and amplitude independent. This has been associated with the Campbell regime. The analysis of this regime is an alternative way to determine  $J_c$  as it has been obtained from the relation between  $J_c$ ,  $\lambda_C$ , and  $h_C$ .

#### ACKNOWLEDGMENTS

Financial support from the Human Capital and Mobility Program on ‘‘Flux pinning in high temperature superconductors’’ and from FOM is acknowledged. L.A.A. is grateful to CAI and CICYT (HAT95-0921-C02-01 and 02) for additional financial support.

- 
- <sup>1</sup>C. P. Bean, Phys. Rev. Lett. **8**, 250 (1962); Rev. Mod. Phys. **36**, 31 (1964).
- <sup>2</sup>J. R. Clem, in *Magnetic Susceptibility of Superconductors and Other Spin Systems*, edited by R. A. Hein *et al.* (Plenum, New York, 1991), p. 177.
- <sup>3</sup>M. Däumling and D. C. Larbalestier, Phys. Rev. B **40**, 9350 (1989).
- <sup>4</sup>E. H. Brandt, Phys. Rev. B **50**, 4034 (1994).
- <sup>5</sup>P. N. Mikheenko and Yu. E. Kuzovlev, Physica C **204**, 229 (1993).
- <sup>6</sup>J. Zhu, J. Mester, J. Lockhart, and J. Turneaure, Physica C **212**, 216 (1993).
- <sup>7</sup>J. R. Clem and A. Sánchez, Phys. Rev. B **50**, 9355 (1994).
- <sup>8</sup>J. Z. Sun, M. J. Scharen, L. C. Bourne, and J. R. Schrieffer, Phys. Rev. B **44**, 5275 (1991).
- <sup>9</sup>H. R. Kerchner, J. Low Temp. Phys. **34**, 33 (1978).
- <sup>10</sup>P. H. Kes, J. Aarts, J. van den Berg, C. J. van der Beek, and J. A. Mydosh, Supercond. Sci. Technol. **1**, 242 (1989).
- <sup>11</sup>P. Koorevaar, J. Aarts, P. Berghuis, and P. H. Kes, Phys. Rev. B **42**, 1004 (1990).
- <sup>12</sup>A. Duarte, E. Fernandez Righi, C. A. Bølle, F. de la Cruz, P. L. Gammel, C. S. Oglesby, B. Bucher, B. Batlogg, and D. J. Bishop, Phys. Rev. B **53**, 11 336 (1996).
- <sup>13</sup>A. I. Larkin and Yu. N. Ovchinnikov, J. Low Temp. Phys. **34**, 409 (1979).
- <sup>14</sup>G. D’Anna, M.-O. André, W. Benoit, E. Rodríguez, D. S. Rodríguez, J. Luzuriaga, and J. V. Wasczak, Physica C **218**, 238 (1993).
- <sup>15</sup>S. Bhattacharya and M. J. Higgins, Phys. Rev. Lett. **70**, 2617 (1993).
- <sup>16</sup>C. Tang, X. Li, S. Bhattacharya, and P. M. Chaikin, Europhys. Lett. **35**, 597 (1996).
- <sup>17</sup>P. Berghuis and P. H. Kes, Phys. Rev. B **47**, 262 (1993).
- <sup>18</sup>S. Bhattacharya and M. J. Higgins, Phys. Rev. B **52**, 64 (1995).
- <sup>19</sup>W. Xing, B. Heinrich, J. Chrzanowski, J. C. Irwin, H. Zhou, A. Cragg, and A. A. Fife, Physica C **205**, 311 (1993).
- <sup>20</sup>B. E. Brown and D. Y. Beernsten, Acta Crystallogr. **18**, 31 (1965).
- <sup>21</sup>L. Civale, T. K. Worthington, L. Krusin-Elbaum, and F. Holtzberg, in *Magnetic Susceptibility of Superconductors and Other Spin Systems* (Ref. 2), p. 313.
- <sup>22</sup>P. de Trey, S. Gygax, and J. P. Jan, J. Low Temp. Phys. **11**, 421 (1973).
- <sup>23</sup>J. Giapintzakis, R. L. Neiman, D. M. Ginsberg, and M. A. Kirk, Phys. Rev. B **50**, 16 001 (1994).
- <sup>24</sup>G. D’Anna, M.-O. André, and W. Benoit, Europhys. Lett. **25**, 539 (1994).
- <sup>25</sup>J. M. E. Geers (private communication).
- <sup>26</sup>M. Marchevsky (private communication).
- <sup>27</sup>G. Blatter, M. V. Feigelman, V. B. Geshkenbein, A. I. Larkin, and V. M. Vinokur, Rev. Mod. Phys. **66**, 1125 (1994).
- <sup>28</sup>A. de Graaf and B. Janossy (private communication).
- <sup>29</sup>V. M. Vinokur, P. H. Kes, and A. E. Koshelev, Physica C **248**, 179 (1995).
- <sup>30</sup>P. H. Kes and R. Wördenweber, J. Low Temp. Phys. **67**, 1 (1987).
- <sup>31</sup>S. Bhattacharya and M. J. Higgins, Physica C **257**, 232 (1996).
- <sup>32</sup>C. J. van der Beek, V. B. Geshkenbein, and V. M. Vinokur, Phys. Rev. B **48**, 3393 (1993).
- <sup>33</sup>A. M. Campbell, J. Phys. C **2**, 1492 (1969).
- <sup>34</sup>E. H. Brandt, Phys. Rev. B **50**, 13 833 (1994).